Transition from Viscous to Elastic-Based Dependency of Mechanical Properties of Self-Assembled Type I Collagen Fibers

FREDERICK H. SILVER, DAVID L. CHRISTIANSEN, PATRICK B. SNOWHILL, YI CHEN

Department of Pathology and Laboratory Medicine, UMDNJ—Robert Wood Johnson Medical School, Piscataway, New Jersey 08854

Received 1 September 1999; accepted 22 February 2000

ABSTRACT: Fibrous collagen networks are the major elements that provide mechanical integrity to tissues; they are composed of fiber forming collagens in combination with proteoglycans and elastic fibers. Using uniaxial incremental tensile stress–strain tests we have studied the viscoelastic mechanical properties of self-assembled collagen fibers formed at pHs between 5.5 and 8.5 and temperatures of 25 and 37°C. Fibers formed at pH 7.5 and 37°C and crosslinked by aging at 22°C and 1 atmosphere pressure were also tested. Analysis of the mechanical tests showed that the ultimate tensile strength (UTS), and slopes of the total, elastic and viscous stress–strain curves were related directly to the volume fraction of polymer. Further analysis suggested that the UTS, and slopes of the total, elastic, and viscous stress–strain curves showed the highest correlation coefficient with the calculated effective fibril length and axial ratio. The mechanical data suggested that at low levels of crosslinking the mechanical properties were dominated by the viscous sliding of collagen molecules and fibrils by each other, which appears to be dependent on the collagen fibril length and axial ratio, while at higher levels of crosslinking the mechanical behavior is dominated by elastic stretching of the nonhelical ends, crosslinks, and collagen triple helix. The latter behavior appears to be dependent on the presence of crosslinks that stabilize fibrillar units. These results lead to the hypothesis that early in development viscous sliding of fibrils plays an important role in the mechanical response of animal tissues to forces experienced *in utero,* while later in development when locomotion is required, mechanical stability is primarily a result of elastic deformation of the different parts of the collagen molecule within crosslinked fibrils. © 2000 John Wiley & Sons, Inc. J Appl Polym Sci 79: 134–142, 2001

Key words: viscoelasticity; collagen fibrils; tendon; axial ratio

INTRODUCTION

Fibrous collagen is the major mechanical element found in tissues and is composed of fiber-forming collagens (types I–III) and proteoglycans.[1] Tendons and ligaments are composed primarily of fiber-forming types I and III collagens, and function to transmit and dissipate loads, and store elastic strain energy applied to the joints of the body.[1–3] The mechanical properties of these tissues change during development and aging, which changes the efficiency by which these functions can occur.[4–13] The consequences of pathobiological changes to tendons and ligaments include joint laxity, instability, and premature mechanical failure.

Correspondence to: F. H. Silver.

Journal of Applied Polymer Science, Vol. 79, 134–142 (2001)

Tendon and ligaments are multiunit hierarchical structures that contain fibrils, fibril bundles, fascicles, and tendon units that run parallel to the geometrical axis.[6–9] The role of extrafibrillar proteoglycans in the structural stability of tendon has been studied extensively by Scott.[14] Proteoglycans and hyaluronan are modeled to swell the aqueous spaces between fibrils limiting tissue collapse.[14] Small proteoglycans including decorin are thought to be tissue organizers, orienting and ordering collagen fibrils.[14] In mature tendon, proteoglycan filaments are seen to be orthogonally arranged in the matrix surrounding collagen fibrils in every D period, suggesting that these elements are involved in force transmission.[15–17]

The stress–strain curve of tendon and ligament is characterized by a low-strain nonlinear "toe region," a linear region, and a nonlinear yield and failure region.[10] The low-strain toe region has been shown to involve the uncrimping of collagen fibrils and fibers,[11,12] as well as initiation of stretching of the triple helix, nonhelical ends, and crosslinks.[18] In the linear region, molecular stretching and molecular and fibrillar slippage are the predominate modes of deformation. These processes lead to defibrillation and failure in the yield and failure region[1,4] after crosslinks between the fibrils break.

The self-assembly of collagen molecules into rigid gels was observed at neutral pH in the 1950s.[19] It was later shown that self-assembly of type I collagen molecules in fiber formation buffer (FFB) under optimum conditions led to the formation of collagen fibrils, with the native 67 nm repeat referred to as the D period.[20] Subsequent studies showed that coextrusion of collagen molecules and FFB led to the formation of D periodic collagen fibers[17,21] that had fibrillar substructure.[17] These fibers can be artificially crosslinked by storage at 22°C and atmospheric pressure for periods between 1 and 6 months.[22]

The purpose of this study is to evaluate the influence of collagen self-assembly conditions on the mechanical properties of collagen fibers in an effort to understand the molecular phenomena that contribute to the macroscopic mechanical behavior of tendons. In this paper we report on the relationship between calculated effective fibril length and axial ratio (ratio of fibril length to width) and the elastic and viscous components of the mechanical behavior of self-assembled collagen fibers.

MATERIALS AND METHODS

The viscoelastic behavior of self-assembled collagen fibers were examined in this study. These fibers were self-assembled from solutions of type I collagen molecules obtained from rat tail tendon (RTT). RTT fibers were obtained from White Sprague–Dawley female rats that weighed 350 $\pm$ 25 g at sacrifice. The tails were freed from skin and washed with distilled water at room temperature. Tendons were removed by gripping the tail with a wire stripper and pulling the fibers from the tail. Tendon fibers were repeatedly teased until the fiber diameter was about 100 μm.

Self-assembled collagen fibers were obtained by extrusion of soluble rat tail tendon collagen as discussed previously.[17] Solutions of soluble type I collagen were obtained by acid extraction of rat tail tendon fibers in 0.01*M* HCl at 4°C overnight. The resulting collagen was centrifuged, salt precipitated, redisolved in 0.01*M* HCl, filtered through 0.65 and 0.45 μm filters, dialyzed against phosphate buffer, and redisolved in 0.01*M* HCl.[17] Collagen fibers were formed by extrusion of collagen solutions in 0.01*M* HCL through a dual barrel syringe system containing the collagen solution in one barrel and FFB in the other barrel.[17] The two solutions were extruded through 18 gauge poly(ethylene) tubing into a container filled with FFB at 37°C, at pHs between 5.5 and 8.5. FFB was removed after 24 h of incubation and replaced with a fiber incubation buffer (FIB) pH 7.4.[17] The fibers were allowed to incubate for an additional 24 h at 37°C, washed with distilled water for 1 h and then air dried under a slight tension for an additional 24 h. Some of the dried fibers were then processed for immediate mechanical testing while others were allowed to age at 22°C for periods of up to 6 months.[22] Fibers for mechanical testing were mounted on vellum "windows" in the same manner as were rat tail tendon fibers; fiber diameters were measured using a microscope with a calibrated eye piece. Collagen fibril diameters were determined from electron microscopy of transverse sections of collagen fibers as described previously.[17]

Standard stress–strain measurements and viscoelastic testing were conducted on wet samples using a hydration chamber at room temperature. Self-assembled collagen fibers were clamped into the hydration chamber, which in turn was placed in the grips of an Instron Model 1122 materials testing machine.[17] Prior to testing, the vellum "window" was cut. In uniaxial tensile tests the

samples were stretched to failure at a strain rate of 50%/min and standard stress–strain data were collected on the Instron. All strains were determined by the displacement of the cross head. Ultimate tensile stresses (UTS) were tabulated from stress–strain measurements. Specimens for viscoelastic testing were subjected to 5% strain increments at a strain rate of 10%/min, resulting in an incremental stress vs strain curve. After each strain increment, the stress was allowed to decay until it remained unchanged for 10 min before an additional strain increment was added. The elastic component of the stress was defined as the stress at equilibrium while the viscous component was calculated from the difference between total stress and the elastic component. Total, elastic, and viscous stress–strain curves were approximated by straight lines using a curve fitting program within Cricket Graph. Correlation coefficients, CC, were generated by the program for the different materials. Elastic fractions were defined as the ratio of the stress at equilibrium to the total stress.[22]

Lines representing the viscous stress–strain curves obtained from incremental stress–strain curves were converted into fibril lengths based on estimation of ratio of fibril length to width (axial ratio) and shape factors[1] in the following manner. Viscous stress–strain equations were approximated by straight lines as discussed above and the equations were divided by the strain rate (0.1/min) to give an equation that represented the extensional viscosity vs strain in MPa-s. The shear viscosity as a function of strain was then approximated from the extensional viscosity by dividing by a value of 3.0, which is equivalent to the relationship between shear modulus and tensile modulus for isotropic materials with Poisson's ratio equal to 0.5.[23] This assumption assumes that the material is incompressible. Shear viscosity as a function of strain was converted into the shape factor V by dividing by the solvent viscosity (8.23×10^{-4} MPa-s) for water and by dividing by the volume fraction of polymer.[1] The volume fraction of polymer was estimated by calculating the ratio of the square of the dry fiber diameter to the square of the wet fiber diameter. It was assumed that the length change was negligible during hydration. The axial ratio Z was estimated from eq. (1) where k is 0.1395 for collagen based on intrinsic viscosity measurements.[17] It should be noted that eq. (1) is typically

$$Z = (V/k)^{0.552} \quad (1)$$

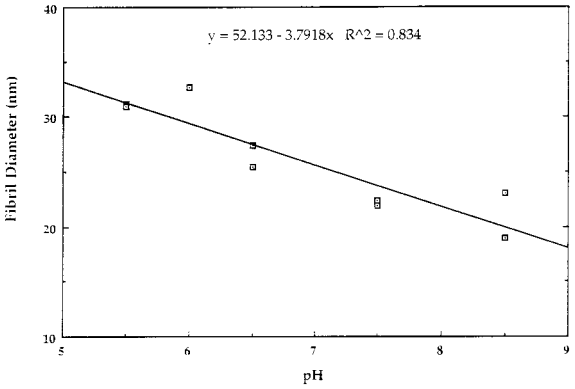

Figure 1 Fibril diameter vs self-assembly pH. Plot of fibril diameter for self-assembled type I collagen fibrils vs pH of fiber formation buffer. Note all fibers are treated with fiber incubation buffer at neutral pH after treatment at various pHs in fiber formation buffer prior to fibril diameter measurements. The equation shown is that of the best fit straight line. $R \hat{} 2$ is the value of the correlation coefficient.

used to calculate the axial ratio from the viscosity of a polymer solution where the polymer is rod shaped or a prolate ellipsoid (see ref. 1). In this case, eq. (1) is used to estimate the viscosity that is associated with the viscous sliding of fibrils in a swollen tissue. The value of Z can be used to interpret the mechanism of strain-dependent viscosity measurements made on self-assembled collagen fibers.

RESULTS

Collagen fibril diameters were varied by changing the pH of the fiber formation buffer during the initiation of fibril formation. However, all fibers were incubated for 24 h in FIB at pH 7.4 prior to preparation for mechanical testing. Fibers self-assembled at acidic pH had larger fibril diameters than fibers self-assembled at neutral or basic pH (Fig. 1). The volume fraction of polymer (ϕ) decreased with increasing pH (Fig. 2), suggesting that the value of polymer volume fraction increased with increasing fibril diameter. UTS was also seen to be directly related to the volume fraction of polymer at low and high values of ϕ [Figs. 3(a) and 3(b)].

Incremental stress–strain curves were measured for self-assembled collagen fibers and found to be approximately linear. Total, elastic, and viscous stress–strain curves were approximated by straight lines (Fig. 4), and the slopes are tabu-

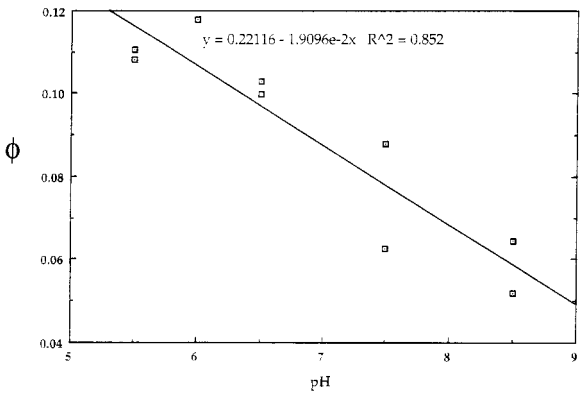

Figure 2 Volume fraction of polymer ϕ vs self-assembly pH. Plot of ϕ vs pH of the fiber formation buffer used to self-assemble type I collagen. The value of ϕ was calculated by taking the ratio of the average dry fibril diameter squared divided by the average wet fibril diameter squared. The equation shown is that of the best fit straight line. R ^ 2 is the value of the correlation coefficient.

lated in Tables I and II. Values of the slopes of the total, elastic, and viscous incremental stress–strain curves were observed to decrease with increasing pH at 25 and 37°C. The values of the slopes increase with increased time of aging at 22°C and atmospheric pressure as is shown by examining Tables I and II. A typical plot of elastic fraction E_f, vs strain shows a logarithmic decrease from an initial value to a baseline value (Fig. 5). Values of the baseline averaged 0.117 for unaged specimens and were above 0.7 for aged specimens.

Values of axial ratio Z and "effective" fibril length l were estimated based on the slope of the viscous stress–strain curve, and are tabulated in Table III. Table IV gives a list of the correlation coefficients obtained when the relationship between different pairs of variables was examined.

When UTS, total slope, elastic slope, and viscous slope were correlated with different parameters, the best correlations were observed with ϕ, l, and Z (Table IV). UTS correlated with fibril diameter but not as strongly as it did with ϕ, l, and Z. Total slope correlated with UTS, elastic slope, and viscous slope as well as with ϕ, l, and Z. Elastic slope correlated with UTS, ϕ, l, Z, and fibril diameter squared.

Plots of UTS and Z (Fig. 6), total slope and ϕ (Fig. 7), total slope and Z (Fig. 8), and viscous slope and Z (Fig. 9) are given as examples. Figures 10(a) and 10(b) show plots of ϕ vs l and Z, respectively.

It was noted that the correlation coefficient between UTS and ϕ and Z increased when both aged and unaged samples were considered in the correlation compared to when only unaged samples were tested. However, when UTS was correlated with l, the coefficient was higher when only unaged samples were used compared to when both unaged and aged samples were tested. The same trend was noted when elastic slope was correlated with ϕ and Z. The viscous slope correlated better with l and ϕ compared to the correlation with Z when both unaged and aged samples were considered.

DISCUSSION

The purpose of this study was to attempt to correlate mechanical properties of self-assembled

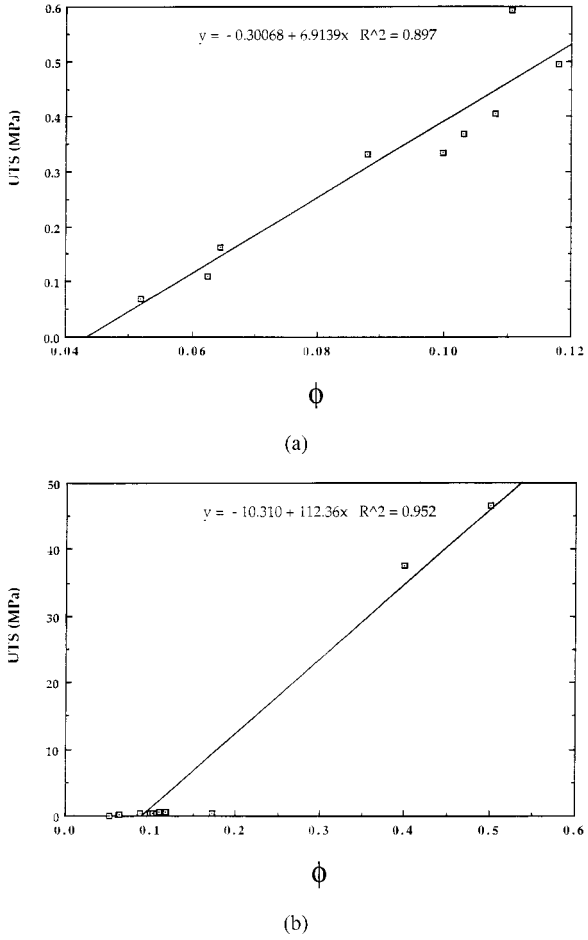

Figure 3 UTS vs volume fraction of polymer ϕ. Plot of UTS vs ϕ for self-assembled type I collagen fibers for values of ϕ less than 0.12 (a) and less than 0.5 (b). The equation shown is that of the best fit straight line. R ^ 2 is the value of the correlation coefficient.

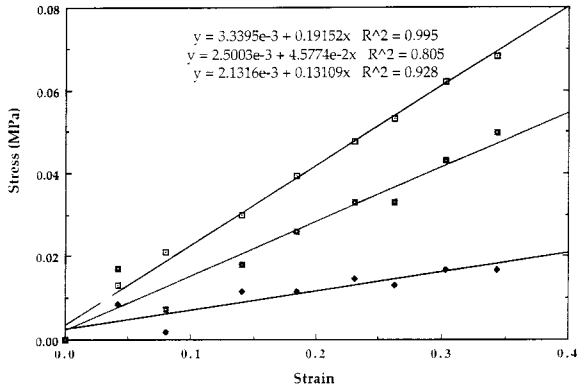

Figure 4 Incremental stress–strain curve for collagen fibers. Total, elastic, and viscous stress–strain curves for unaged self-assembled type I collagen fibers formed at pH 8.5 and 37°C. The total stress–strain curve (open boxes) was obtained by collecting all the initial, instantaneous, force measurements at increasing time intervals and then dividing by the initial cross sectional area. The elastic stress–strain curve (closed diamonds) was obtained by collecting all the force measurements at equilibrium and then dividing by the initial cross sectional area. The viscous component curve (closed squares) was obtained as the difference between the total and the elastic stresses. The equations shown are the best fit straight lines for the total (top), elastic (middle), and viscous (bottom) stress–strain equations. $R \hat{} 2$ is the value of the correlation coefficient.

collagen fibers with structural parameters that can be altered by modification of the fibril formation process. Previous work by Danielsen[24] showed that reconstituted collagen fibrils when dried into films showed a strength gain over time that was attributed to conversion of reducible crosslinks to nonreducible crosslinks suggesting that the extent of crosslinking is important in determining the UTS of a tissue. In contrast, Parry[25] has shown that the UTS of collagenous tissues is directly related to the fibril diameter.

Table II Slopes and Intercepts of Straight Line Approximations For Viscous Stress–Strain Curves For Self-Assembled Type I Collagen Fibers Obtained at a Strain Rate of 10%/min

Sample pH, T (°C)	Straight Line Slope (Intercept) (MPa)	CC[a]	N[a]
5.5, 25	1.139 (0.0058)	0.970	6
6.5, 25	0.744 (−0.0081)	0.993	6
7.5, 25	0.743 (0.0111)	0.972	6
8.5, 25	0.297 (0.0143)	0.958	6
5.5, 37	0.973 (0.0177)	0.980	6
6.5, 37	0.776 (0.0097)	0.989	6
7.5, 37	0.238 (0.0048)	0.974	6
8.5, 37	0.131 (0.0021)	0.928	6
pH 7.5, 37			
Aged 3 months	25.2 (−0.293)	0.861	9
Aged 6 months	45.0 (−0.454)	0.891	10

[a] Denotes correlation coefficient. Note correlation coefficients of 1.0 typically mean that only two strain points were available for slope determination.
[b] N = number of samples tested.

Table I Slopes and Intercepts of Straight Line Approximations For Total and Elastic Stress–Strain Curves For Self-Assembled Type I Collagen Fibers Obtained at a Strain Rate of 10%/min

Sample pH, T (°C)	Total Stress Slope (Intercept) (MPa)	CC[a]	Elastic Stress Slope (Intercept) (MPa)	CC[a]	N[b]
5.5, 25	1.71 (0.0282)	0.964	0.398 (0.0317)	0.909	6
6.5, 25	0.903 (0.0105)	0.994	0.169 (0.184)	0.831	6
7.5, 25	0.960 (0.0246)	0.973	0.190 (0.0115)	0.856	6
8.5, 25	0.353 (0.0306)	0.922	0.0629 (0.0141)	0.571	6
5.5, 37	1.221 (0.0289)	0.982	0.0242 (0.0167)	0.948	6
6.5, 37	0.989 (0.0419)	0.940	0.268 (0.0152)	0.930	6
7.5, 37	0.300 (0.0111)	0.970	0.054 (0.0067)	0.810	6
8.5, 37	0.192 (0.0035)	0.995	0.0458 (0.0051)	0.805	6
7.5, 37					
Aged 3 months	186.7 (−4.85)	1.00	143 (−3.0)	1.00	9
Aged 6 months	394 (−11.51)	1.00	321.7 (−8.77)	1.00	10

[a] Denotes correlation coefficient. Note correlation coefficients of 1.0 typically mean that only two strain points were available for slope determination.
[b] N = number of samples tested.

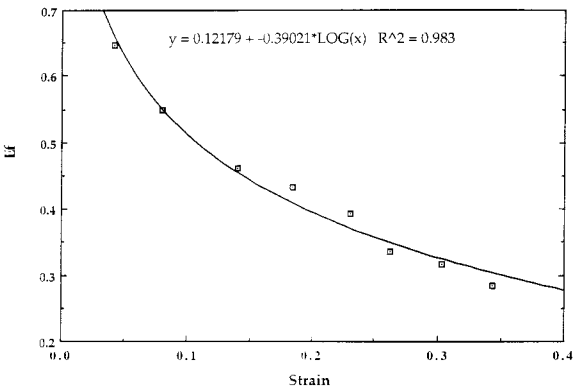

Figure 5 Elastic fraction E_f, vs strain for collagen fibers. Ratio of elastic stress divided by the total stress (E_f) as a function of strain for self-assembled type I collagen fibers formed at pH 8.5 and 37°C. Note the logarithmic decrease in E_f with increasing strain to a baseline value. The equation shown is that of the best fit found to the data. R ^ 2 is the value of the correlation coefficient.

These observations are consistent if fibrils with greater diameters have larger numbers of crosslinks.

Molecular level studies on tendon indicate that up to a strain of 2% stretching of the triple helix is the predominant mechanism for deformation.[26] Beyond 2%, it is believed that molecular stretching and slippage occur, resulting in increases in the D period and the axial rise per residue along the triple helix.[18,26]

Previously[22] we have reported that the slope of the elastic stress–strain curve for rat tail tendons after correction for the ratio of the axial rise per residue divided by the macroscopic strain is consistent with the elastic stiffness or spring constant for collagen type I.[22] The slope of the viscous stress–strain curve appears to reflect interfibrillar shear interactions and can be used to calculate an "effective" fibril length.[22] Crosslinking appears to increase the elastic spring constant and the effective fibril length,[22] although it may also limit the increase in the collagen D period with macroscopic strain.[22]

Results of studies reported in this paper suggest that UTS of self-assembled collagen fibers shows a direct correlation with fibril diameter, but this correlation is not as strong as the correlation between the volume fraction of polymer and UTS. The volume fraction of polymer in turn can be correlated with both the effective fibril length and axial ratio, as is shown in Figures 10(a) and (b). The relationship between the fibril axial ratio and length, the volume fraction of polymer, and the UTS of self-assembled collagen fibers is an interesting observation. UTS is also correlated with the slope of the total stress–strain curve; the total slope appears to be related to Young's modulus obtained from constant strain-rate experiments.[22]

The stress–strain curves for self-assembled collagen fibers reported in this study are almost linear. The linearity is due to the alignment of the fibers that occurs during drying prior to mounting of the fibers on the vellum windows used in mechanical testing.

Table III Estimation of Axial Ratios and Effective Fibril Lengths From The Slope of the Viscous Stress–Strain Curves

Sample pH, T (°C)	Volume Fraction	Axial Ratio[a] Equation Constant	Diameter (nm)	Effective Fibril Length, μm
5.5, 25	0.116	513	31.2	16.0
6.5, 25	0.106	404	25.5	10.3
7.5, 25	0.088	447	22.4	10.0
8.5, 25	0.064	304	18.9	5.80
5.5, 37	0.141	341	31.0	10.6
6.0, 37	0.135	457	32.7	14.9
6.5, 37	0.137	359	27.4	9.84
7.5, 37	0.0625	288	22.4	6.19
8.5, 37	0.052	230	23.1	5.31
7.5, 37				
Aged 3 months	0.402	1352	22.4	30.3
Aged 6 months	0.495	33,200	22.4	39.2

[a] Axial ratio calculated using eq. (1).

Table IV Correlation Coefficients For Linear Relationship Between Different Parameters For Self-Assembled Collagen Fibers

Parameters	Correlation Coefficient: Unaged Samples	Correlation Coefficient: All Samples
UTS, ϕ	0.952	0.897
UTS, Z	0.971	0.971
UTS, l	0.888	0.948
UTS, fibril diameter	0.606	0.606
UTS, fibril diameter^2	0.713	0.713
Total slope, ϕ	0.839	0.908
Total slope, Z	0.939	0.939
Total slope, l	0.860	0.860
Total slope, UTS	0.936	0.936
Total slope, fibril diameter	0.771	0.069
Total slope, fibril diameter^2	0.776	0.776
Total slope, elastic slope	0.999	0.999
Total slope, viscous slope	0.995	0.995
Elastic slope, ϕ	0.827	0.919
Elastic slope, Z	0.596	0.928
Elastic slope, l	0.925	0.850
Elastic slope, fibril diameter	0.069	0.086
Elastic slope, fibril diameter^2	0.708	0.708
Elastic slope, UTS	0.923	0.921
Viscous slope, ϕ	0.933	0.962
Viscous slope, Z	0.965	0.965
Viscous slope, l	0.563	0.888
Viscous slope, fibril diameter	0.064	0.064
Viscous slope, fibril diameter^2	0.775	0.755
Viscous slope, UTS	0.971	0.965

A question that arises in reviewing these results relates to the relationship between volume fraction of polymer, effective fibril length, and axial ratio. This relationship implies that a decrease in swelling due to crosslinking is likely to reflect increases in effective fibril length. Therefore, fibril crosslinking probably reflects formation of end-to-end crosslinks between molecules within a fibril. This would explain the correlation between the slope of the elastic stress–strain curve and the axial ratio and length, as well as the correlation between viscous slope and fibril length and axial ratio. However, it would not explain the correlation between fibril diameter and the slopes of the total and elastic stress–strain curves. It may be hypothesized that the correlation between fibril diameter and UTS reported by Parry[25] reflects the tendency for thicker fibrils to

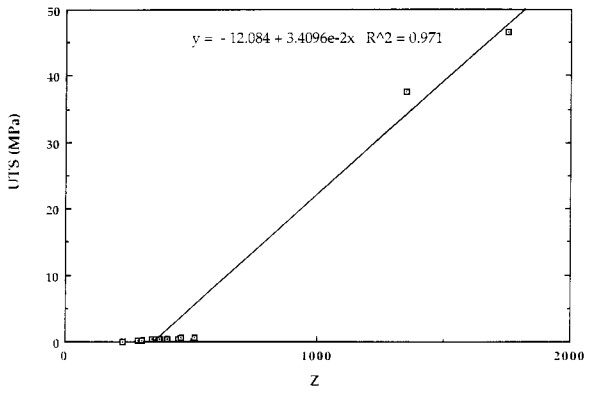

Figure 6 UTS vs axial ratio (Z). Plot of UTS vs Z for unaged and aged self-assembled type I collagen fibers. The equation shown is that of the best fit straight line. R ^ 2 is the value of the correlation coefficient.

have more crosslinks that connect the ends of collagen molecules into long fibrils. If this is the case, then one would expect a correlation to exist between fibril diameter and the length of collagen fibrils in tissues.

The correlation between the viscous slope, effective fibril length, and axial ratio was another interesting observation made during the course of these studies. This paralleled a similar correlation between elastic slope and the same variables. Since both elastic and viscous slopes showed such a strong correlation with fibril length and axial ratio, this suggests that both elastic and viscous mechanisms of deformation are interrelated. Since the elastic component reflects molecular stretching within crosslinked fibrils and the vis-

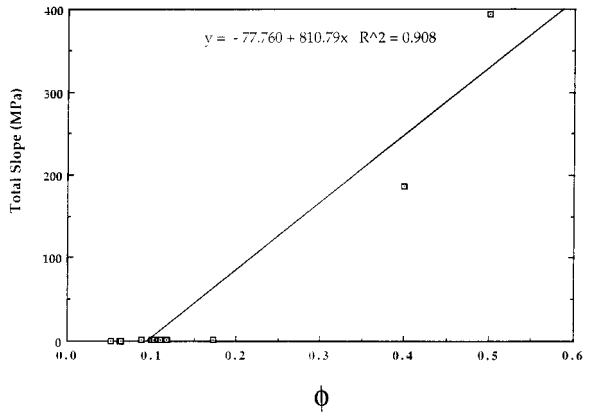

Figure 7 Total slope vs volume fraction of polymer (ϕ). Total slope is plotted vs ϕ for unaged and aged self-assembled type I collagen fibers. The equation shown is that of the best fit straight line. R ^ 2 is the value of the correlation coefficient.

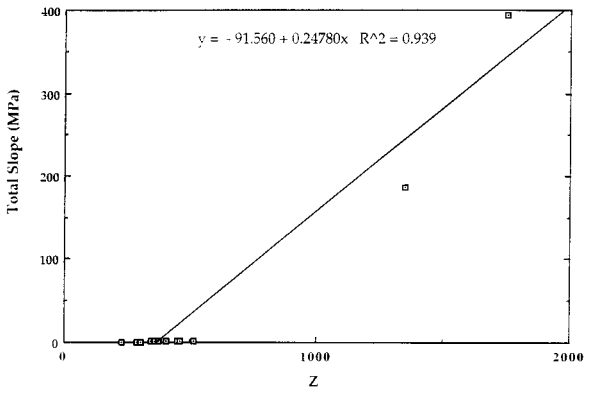

Figure 8 Total slope vs axial ratio (Z). Dependence of total slope on Z for unaged and aged self-assembled type I collagen fibers. The equation shown is that of the best fit straight line. $R \hat{} 2$ is the value of the correlation coefficient.

cous component reflects slippage, then the increased viscous forces associated with increased elastic forces suggests that the structural unit involved in both of these processes is the same and is probably the fibril. This supports the model that fibrils are discontinuous and get longer during crosslinking.

The concept that fibrils are discontinuous is consistent with a previous report on developing chick leg extensor tendon.[5] In that study the UTS of developing chick leg extensor tendon increased from about 2 MPa at embryonic day 14 to 60 MPa 9 days later, after the chick hatched. This large change in UTS was hypothesized to be related to an increase in the fibril length and not to the changes in fibril diameter. The results of this prior study *in vivo,*[5] taken together with the results of the current study on self-assembled collagen fibers, suggest that during early development of chick extensor tendon the mechanical behavior of collagen fibers is dominated by viscous slippage. Under these conditions the UTS is low. After crosslinking occurs primarily at the ends of the molecules within fibrils, the behavior is dominated by elastic deformation of collagen molecules. This increases the UTS and stiffens the tissue.

Previously we have reported for rat tail tendon fibers that the slope of the viscous component is significantly higher than that found for self-assembled collagen fibers that are devoid of proteoglycans even though the slope of the elastic stress–strain curve is not significantly different.[22] This would

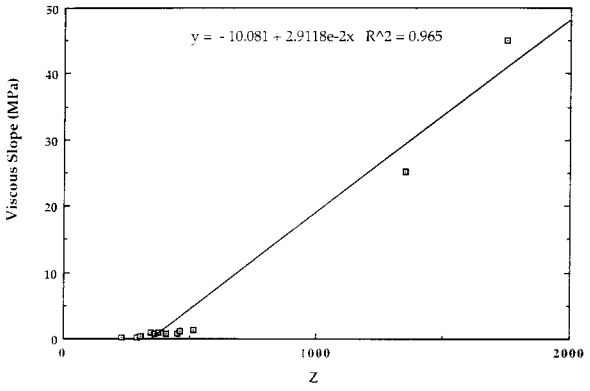

Figure 9 Viscous slope vs axial ratio (Z). Plot of viscous slope vs Z for unaged and aged self-assembled type I collagen fibers. The equation shown is that of the best fit straight line. $R \hat{} 2$ is the value of the correlation coefficient.

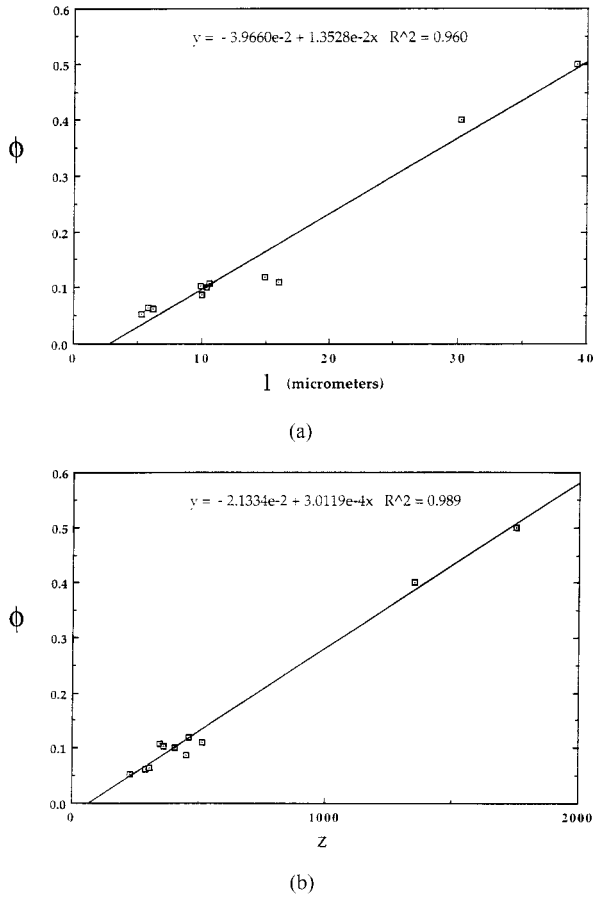

Figure 10 Volume fraction of polymer ϕ vs calculated effective fibril length (l) and axial ratio (Z). Plot of ϕ vs l (a) and Z (b) for unaged and aged self-assembled type I collagen fibers. The equations shown are that of the best fit straight lines. $R \hat{} 2$ is the value of the correlation coefficient.

suggest that interfibrillar shear forces that occur between fibrils are increased by the proteoglycans that are present. The specific binding of decorin to collagen as shown by Scott[14–16] probably enhances the viscous transfer of energy between collagen fibrils during tensile deformation. This would increase the viscous contribution to the stress-bearing capacity of the tendon, and may promote alignment of collagen fibrils enhancing the ability of the tissue to deform before failure.[17]

Finally, the ability of embryonic tissues to exist in a liquid-like viscous state is consistent with the observation of rapid gross and microscopic tissue structural changes that occur during fetal development.[5] In contrast, the formation of crosslinks between the ends of collagen molecules within a fibril is necessary to support the forces required for locomotion and movement of animals after birth. This rapid transition is an interesting example of how nature adapts to meet different mechanical requirements.

The authors would like to acknowledge the assistance of Daniel Behin, a pre-med student enrolled at Rutgers University (Piscataway, NJ), in conducting the mechanical tests.

REFERENCES

1. Silver, F. H. Biological Materials: Structure, Mechanical Properties and Modeling of Soft Tissues; New York University Press: New York, 1987.
2. Alexander, R. M. Animal Mechanics, 2nd ed.; Blackwell Scientific: Oxford, UK, 1983.
3. Alexander, R. M. A Zool 1984, 24, 85–94.
4. Torp, S.; Baer, E.; Friedman, B. Colston Papers 1975, 26, 223–250.
5. McBride, D. J.; Trelstad, R. L.; Silver, F. H. Int J Biol Macromol 1988, 10, 194–200.
6. Elliott, D. H. Biol Rev 1965, 40, 392–421.
7. Greenlee, T. K.; Ross, R. J Ultrastruct Res 1967, 18, 353–376.
8. Rowe, R. W. D. Connect Tissue Res 1985, 14, 9–20.
9. Rowe, R. W. D. Connect Tissue Res 1985, 14, 21–30.
10. Silver, F. H.; Kato, Y. P.; Ohno, M.; Wasserman, A. J. J Long-Term Effects of Medical Implants 1992, 2, 165–198.
11. Rigby, B. J.; Hirai, N.; Spikes, J. D.; Eyring, H. J Gen Physiol 1959, 43, 265–283.
12. Diamant, J.; Keller, A.; Baer, E.; Lith, N.; Arridge, R. G. C. Proc R Soc London Ser B 1972, 180, 293–315.
13. Yahia, L.-H.; Drouin, G. J. Orthopaedic Res 1969, 7, 243–251.
14. Scott, J. E. J Anat 1995, 187, 259–269.
15. Scott, J. E. Biochemistry 1996, 35, 8795–8797.
16. Cribb, A. M.; Scott, J. E. J Anat 1995, 187, 423–428.
17. Pins, G. D.; Christiansen, D. L.; Patel, R.; Silver, F. H. Biophys J 1997, 73, 2164–217.
18. Mosler, E.; Folkhard, W.; Knorzer, E. J Mol Biol 1985, 182, 589–596.
19. Gross, J.; Highberger, J. H.; Schmitt, F. O. Proc Soc Exp Biol Med 1952, 80, 462–465.
20. Gelman, R. A.; Williams, B. R.; Piez, K. A. J Biol Chem 1979, 254, 180–186.
21. Kato, Y. P.; Christiansen, D. L.; Hahn, R. A.; Shieh, S. J.; Goldstein, J. D.; Silver, F. H. Biomaterials 1989, 10, 38–42.
22. Silver, F. H.; Christiansen, D. L.; Snowhill, P. B.; Chen, Y. Connect Tissue Res 2000, 41, 155–164.
23. Cowin, S. C. In Bone Mechanics; Cowin, S. C., Ed.; CRC Press: Boca Raton, FL, 1989; Chap 2.
24. Danielsen, C. C. Connect Tissue Res 1982, 9, 219–225.
25. Parry, D. A. D. Biophys Chem 1988, 29, 195–209.
26. Sasaki, N.; Odajima, S. J. Biomech 1996, 29, 655–658.
27. McBride, D. J.; Hahn, R.; Silver, F. H. Int J Biol Macromol 1985, 7, 71–76.